Eur. Phys. J. C 11, 709–715 (1999)
Digital Object Identifier (DOI) 10.1007/s100529900077

THE EUROPEAN
PHYSICAL JOURNAL C

Nucleon time-like form factors below the $\mathrm{N\overline{N}}$ threshold

R. Baldini[1], S. Dubnička[2], P. Gauzzi[3], S. Pacetti[1], E. Pasqualucci[3], Y. Srivastava[4]

[1] INFN Laboratori Nazionali di Frascati, Italy
[2] Ist. of Physics, Slovak Acad. of Sciences, Bratislava, Slovakia
[3] Dipartimento di Fisica dell'Università and INFN, Roma "La Sapienza", Italy
[4] Dipartimento di Fisica dell'Università and INFN, Perugia, Italy

Received: 20 January 1999 / Published online: 3 November 1999

Abstract. The nucleon magnetic form factors in the unphysical region, i.e., for time-like Q^2 but below the $\mathrm{N\overline{N}}$ threshold, have been obtained by means of dispersion relations in a model-independent way, without any bias towards expected resonances. Space-like and time-like data have been employed, along with a regularization unfolding method to solve the integral equation. Remarkably, resonance structures with peaks for the $\rho(770)$ and $\rho'(1600)$ and a structure near the $\mathrm{N\overline{N}}$ threshold are automatically generated. The obtained ρ has a much larger width, whose significance is explored. No evidence is found for a peak at the Φ mass, in spite of the expectation that such a peak exists when there is a sizeable polarized $\mathrm{s\bar{s}}$ content in the vector current of the nucleon.

Introduction

Nucleon spectral functions and electromagnetic form factors (FF) play a fundamental role in our understanding of the hadronic dynamics. Hence, for over 30 years, many attempts have been made through dispersion relations (DR) [1–3, 8, 9, 12] to unravel the spectral functions and the FF in the time-like region, in particular for unphysical Q^2 below the $\mathrm{N\overline{N}}$ threshold. In principle, spectral functions and FF in the time-like region may be computed via DR from the measurements of the space-like FF only [12]. However, this is an ill-posed mathematical question, because the answer depends in an unstable way on the input data, and an impossible accuracy is needed to get a unique, stable solution [12, 13]. Up to now, most of the FF evaluations in the time-like region have been done under the assumption of the vector dominance model (VDM) [4], unitarized VDM [5], or in the framework of the Skyrme model [6, 7]. The lack of data on $\mathrm{e^+e^-} \to \mathrm{N\overline{N}}$ had prevented much progress in this endeavor.

Recently, measurements of the proton time-like magnetic FF have been done on a large Q^2 interval [14, 15] and, even more recently, data concerning the neutron time-like FF have also become available [16]. These data turn out to be quite different from QCD expectations [17, 18]. In particular, it has been shown that the neutron time-like magnetic FF measurements are twice those predicted by a dispersive approach [9], assuming perturbative QCD (PQCD) asymptotic behaviors and a reasonable model for unphysical Q^2. Different conclusions have been achieved on the basis of a unitarized VDM [10]. Yet the discrepancy is large enough to prompt further measurements of the neutron time-like FF [9], and new proposals toward this purpose are under way [19]. Pending future experiments, let us explore some implications of the available experimental data, through a consideration of several open questions:

- A sizeable, polarized, $\mathrm{s\bar{s}}$ content in the nucleon has been suggested a long time ago and has been resumed to interpret sum rules violations in deep inelastic scattering of polarized leptons on polarized nucleons [20]; an $\mathrm{s\bar{s}}$ content is also suggested by the nucleon sigma term and other measurements [21]. The evidence, or lack thereof, of a sizeable Φ peak in the nucleon magnetic FF in the unphysical region, obtained in a model-independent way, would be a very direct check of a polarized $\mathrm{s\bar{s}}$ content in the vector current.
- At high Q^2, the neutron time-like magnetic FF is found to be larger than that for the proton, while one had expected it to be – as in the space-like region – $\sim 1/2$ of the proton magnetic FF [17, 18]. This indicates some nontrivial dynamical activity in between.
- At high Q^2, the size of the time-like proton magnetic FF itself is somewhat unexpected, since it is twice the value of its space-like FF counterpart at the same $|Q^2|$. We note that PQCD [22] and analyticity [23] predict both to be asymptotically the same.
- Below threshold, there are indications for narrow structures in the total σ ($\mathrm{e^+e^-} \to$ hadrons) cross section [24], suggested also by the proton and the neutron FF. These may be related to similar effects in $\mathrm{\bar{p}d}$ annihilation in odd and even C channels [25] and suggest a close investigation of the FF just below threshold (in principle, such is feasible experimentally, through a very high statistics analysis of the reaction $\mathrm{p\bar{p}} \to \mathrm{e^+e^-\pi^0}$ [26]).

– FF phases are needed to interpret anomalies in J/$\Psi \to$ hadrons [27].

In the present work, we shall assume that the available data are indeed reliable, and we shall use them as input to evaluate the FF for unphysical Q^2. To make our results as model-independent as possible, *we do not bias our analysis towards expected resonances*. Instead, we let resonance structures and phases arise directly from the solution of the DR. In contrast with the past, presently the nucleon FF are unknown in a limited interval only. Thus, continuity through the interval limits can be implemented. Hence the concerns mentioned above about a stable evaluation may be relieved, being an interpolation rather than an analytical continuation. Unfortunately, present accuracy is still not sufficient to provide a unique solution. Until even better time-like data become available, we seek a solution under an additional smoothness hypothesis, implementing the regularization method described below.

1 Solving DR by means of a regularization method

In order to get a form factor $G(Q^2)$ for $0 < Q^2 < 4M_N^2$ (with Q^2 defined to be positive in the time-like region), DR for $\log G(Q^2)$ are considered [1]. The quantity $\log G(Q^2)$, just as $G(Q^2)$, is analytic on the first sheet of the complex Q^2 plane, with the same cuts on the real positive axis and with additional poles where the FF has zeros. In the following, we shall assume the absence of zeros (in FF) on the first sheet. This hypothesis will be discussed later.

The DR relates the space-like $\log G(Q^2)$ to the time-like $\log|G(Q^2)|$. After making a subtraction at $Q^2 = 0$, we have [1]:

$$\log G(Q^2) = \frac{Q^2\sqrt{Q_0^2 - Q^2}}{\pi}\int_{Q_0^2}^{\infty}\frac{\log|G(t)|}{t(t-Q^2)\sqrt{t-Q_0^2}}\mathrm{d}t \tag{1}$$

where $Q_0^2 = 4m_\pi^2$.

Once $\log|G(Q^2)|$ has been determined, the FF phase $\delta(Q^2)$ for time-like Q^2 is given by:

$$\delta(Q^2) = -\frac{Q^2\sqrt{Q^2 - Q_0^2}}{\pi}\,\mathrm{Pr}\int_{Q_0^2}^{\infty}\frac{\log|G(t)|}{t(t-Q^2)\sqrt{t-Q_0^2}}\mathrm{d}t \tag{2}$$

By splitting the integral in (1) into two parts, $\int_{Q_0^2}^{\infty} = \int_{Q_0^2}^{Q_1^2} + \int_{Q_1^2}^{\infty}$, where $Q_1^2 = 4M_N^2$ is the upper boundary of the unphysical region, one can separate the unphysical region, in which the FF are unknown, from the experimentally accessible region. In this way, an integral equation of the first kind, linear in the unknown $\log|G|$, can be derived from the DR:

$$\log G(Q^2) - I(Q^2) = \frac{Q^2\sqrt{Q_0^2 - Q^2}}{\pi} \times \int_{Q_0^2}^{Q_1^2}\frac{\log|G(t)|}{t(t-Q^2)\sqrt{t-Q_0^2}}\mathrm{d}t \tag{3}$$

where

$$I(Q^2) = \frac{Q^2\sqrt{Q_0^2 - Q^2}}{\pi}\int_{Q_1^2}^{\infty}\frac{\log|G(t)|}{t(t-Q^2)\sqrt{t-Q_0^2}}\mathrm{d}t. \tag{4}$$

This integral is a known quantity that can be calculated directly from the experimental data in the time-like region with some recipe to extrapolate them to very high Q^2.

In order for instabilities in solving (3) to be avoided, a regularization technique exploiting smoothness has to be applied [13]. These techniques have been applied mostly in the unfolding of a spectrum affected by a finite resolution, to avoid the instability usually met in solving first-kind integral equations. The procedure adopted here is as follows:

– $I(Q^2)$ has been calculated by fitting of the time-like data to a rational, smooth function having the expected asymptotic behavior. The subtraction at $Q^2 = 0$, as usual, helps in making the results less dependent on the asymptotic extrapolation.
– A special treatment is adopted near the N$\overline{\text{N}}$ threshold: The upper boundary of the unphysical region has been shifted to $Q_2^2 = Q_1^2 + \Delta$, with $\Delta \simeq 0.5$ GeV^2, in order that instabilities that may originate from steep threshold behavior of the nucleon FF can be avoided. A new DR is then considered for the region (Q_1^2, Q_2^2) as described in Sect. 3.
– Continuity of the function through the upper boundary of the unphysical region is imposed. At the lower boundary, $4m_\pi^2$, only a very mild continuity is demanded, in order to allow any steep variation.
– A regularization is finally introduced by the requirement that the total curvature of the FF in the unphysical region, $r = \int_{Q_0^2}^{Q_2^2}\left((\mathrm{d}^2|G(t)|)/(\mathrm{d}t^2)\right)^2\mathrm{d}t$, be limited. Instead of the second derivative of $\log|G|$, as in the standard procedure [13], the second derivative of $|G|$ has been chosen for this purpose; the reason is that fluctuations in $|G|$ are important only when $|G|$ is large, while $\log|G|$ fluctuations would be important when $|G|$ is small also.

A linearization method has been used to solve (3): The integrals have been transformed into sums over $M = 50$ suitable subintervals in Q^2, with their widths increasing with Q^2. This is tantamount to a further smoothness hypothesis, effectively integrating over any structure whose half width is narrower than a minimum of about 50 MeV.

The integral over the j^{th} subinterval has been approximated by

$$F_j\int_{T_j}^{T_{j+1}}\frac{\mathrm{d}t}{t(t-Q^2)\sqrt{t-Q_0^2}} \tag{5}$$

where $F_j = \log|G[(T_{j+1} + T_j)/2]|$ is the function calculated in the middle of the subinterval with boundaries at T_j and T_{j+1}.

The integral equation (3) is then solved by minimization of the quantity:

$$R_{\mathrm{tot}} = \sum_{i=1}^{L} \left\{ \sum_{j=1}^{M} F_j \frac{Q_i^2 \sqrt{Q_0^2 - Q_i^2}}{\pi} \times \int_{T_j}^{T_{j+1}} \frac{\mathrm{d}t}{t(t-Q_i^2)\sqrt{t-Q_0^2}} + I(Q_i^2) - \log(G(Q_i^2)) \right\}^2 + \tau^6 r(\mathrm{e}^{F_j}) \qquad (6)$$

where the F_j are free parameters and Q_i^2, with $i = 1, ..., L$, corresponding to experimental points available in the space-like region.

The dumping parameter τ has to be set experimentally. It will not respond to sharp structures if it is set too large, whereas unstable solutions will found if too small a value is used.

The uncertainties in the solution of (2) and (3), due to the experimental errors, have been evaluated by the simulation of new sets of space-like and time-like data, according to the quoted errors, and the solution of the DR for each simulated data set.

2 Test of the regularization method

To test the whole procedure and get a suitable range for the τ parameter, we selected the pion FF. In the time-like region, this FF is known up to the J/Ψ mass and at higher Q^2 is extrapolated according to first-order PQCD prescriptions [22]. Pion space-like FF has been reobtained in two ways: (i) according to (1), from the time-like data and (ii) according to the unsubtracted DR. The latter is in fair agreement with present space-like data, as is shown in Fig. 1a. Their difference is most likely due to the uncertainty in the data above the ρ and in the asymptotic extrapolation, as is indicated by the effect of the inclusion of a subtraction. This agreement also provides a check that there are no relevant zeros in the isovector FF. This check would have been airtight were the pion space-like FF data for high Q^2 not obtained through extrapolations of the pion electroproduction data.

So that the τ parameter will be fixed, the space-like dashed area, achieved by means of (1), and the time-like dashed area, obtained by fitting of the data above $Q_2^2 = 4.0\ \mathrm{GeV}^2$, have been used as input in (6) to retrieve the time-like pion FF in the region between Q_0^2 and Q_2^2. It turns out that $\tau \sim M_\pi$ is a suitable value to recover quite satisfactorily the ρ peak, the ρ width, and also the dip at 1.6 GeV, as shown in Fig. 2. It is worthwhile stressing that, in solving the DR, steep structures like the ρ and even the interference pattern beyond the ρ are well retrieved from smooth inputs, once these inputs are built from these structures.

The phase of the pion FF, from the solution of (2), is shown in Fig. 3. Its expected asymptotic value of 180 degrees is already reached above ~ 2 GeV [27].

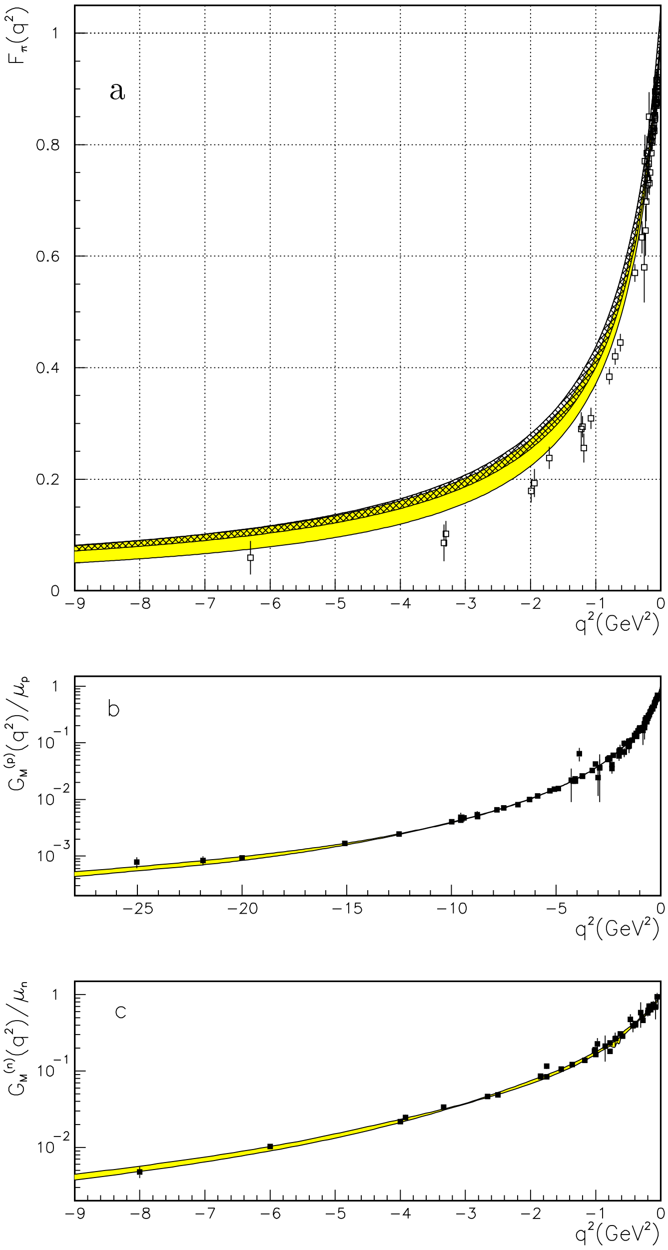

Fig. 1. a Space-like pion **a**, proton magnetic **b** and neutron magnetic **c** form factor from DR applied to time-like data. In **a** the results with and without (dashed area) subtraction are compared

3 The proton time-like magnetic FF

Some comments are in order about the hypotheses governing the extraction of the proton FF from cross section measurements. It has been assumed that at threshold there is only one FF, because $G_M(4M_N^2) = G_{\mathrm{E}}(4M_N^2)$, assuming analyticity for electric and magnetic FF as well as for the Pauli and Dirac FF, i.e. that exactly at threshold, there is only an S wave. Data are consistent with this hypothesis. Furthermore, at high Q^2, the contribution of G_{E} to the total cross section is dumped by a factor $4M^2/Q^2$. In

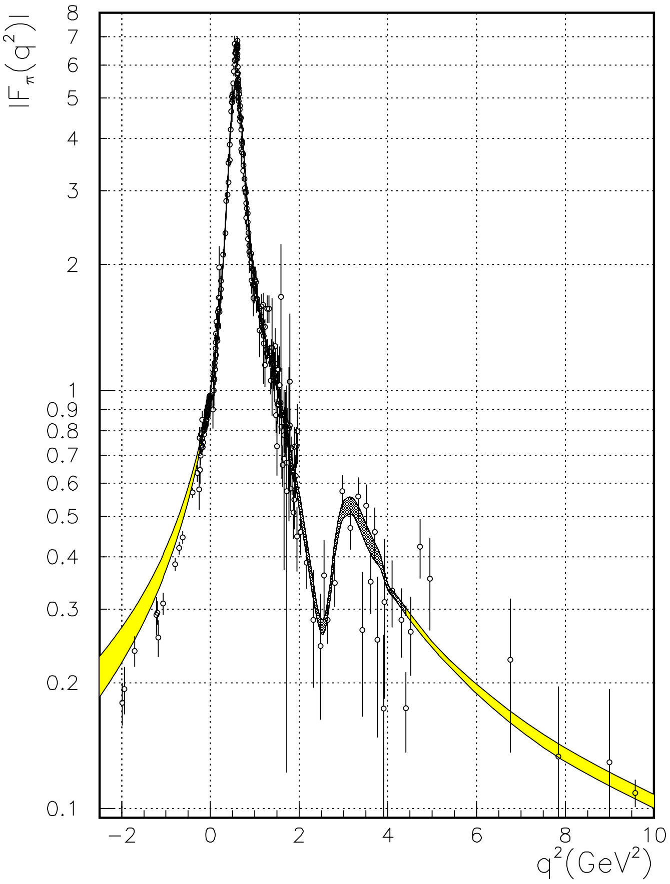

Fig. 2. Pion form factor. The black shaded area is the solution of (6), the gray shaded area is the input of the equation

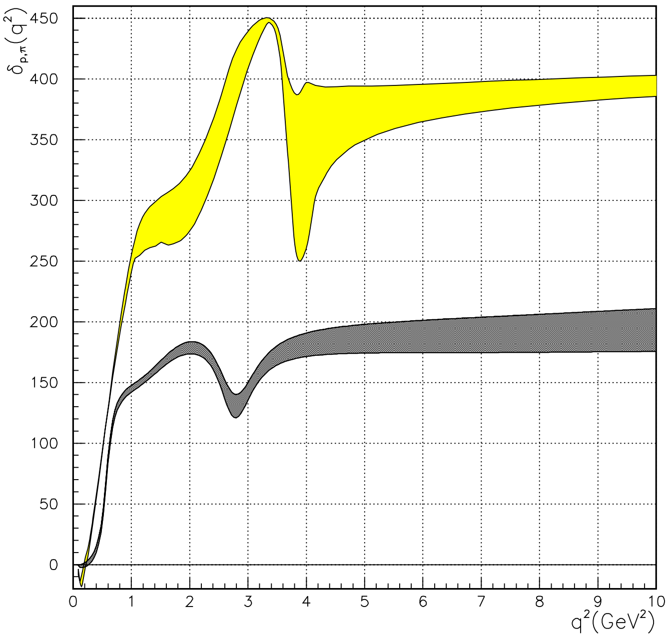

Fig. 3. Phase of pion (black shaded) and proton magnetic (gray shaded) form factor according to (2)

conclusion, in the whole range explored, what is actually measured is very likely to be G_M.

$G_M^{\rm p}$ seems to reach its expected asymptotic behavior $1/Q^4$ quite precociously, but it is higher by a factor of 2 than $G_M^{\rm p}$ at the same space-like $|Q^2|$, whereas asymptotically, they should be equal [23]. Therefore, an asymptotic extrapolation done according to PQCD may be suspect. Yet it has been checked that all the achieved results are quite insensitive to the details of this extrapolation.

Very near threshold, the data show a steep variation [15], beyond Coulomb enhancement (which has already been corrected in the data). In the following, this steep rise has been assumed to affect the FF in a limited Q^2 region, below and above the threshold. This is the reason for choosing $Q_2^2 = 4M_N^2 + \varDelta$ as upper limit in (3). G_M and the first two derivatives are supposed to be continuous functions through this upper limit.

Once a FF G_0 has been determined from (6), another DR is considered in the interval $[Q_1^2 - \varDelta, Q_1^2 + \varDelta]$:

$$\frac{Q^2}{\pi}\int_{Q_1^2-\varDelta}^{Q_1^2}\frac{\log|G_1(t)|}{t(t-Q^2)\sqrt{t-Q_0^2}}\mathrm{d}t + \frac{Q^2}{\pi}\int_{Q_1^2}^{Q_1^2+\varDelta}\frac{\log|G_1(t)|}{t(t-Q^2)\sqrt{t-Q_0^2}}\mathrm{d}t = 0 \qquad (7)$$

where G_1 is determined from the relation: $G_M = G_0 G_1$ in this interval and $G_M = G_0$ outside. Finally, the proton magnetic FF in the unphysical region as obtained by our procedure is reported in Fig. 4a.

The most striking feature of Fig. 4a is the evidence for two resonances, not built in *a priori*, at $M \sim 770$ MeV and $M \sim 1600$ MeV. It is most satisfying to deduce the presence of $\rho + \omega$ and of $\rho' + \omega'$ exactly as expected. On the other hand, the width of the bump at the ρ mass is ~ 350 MeV, to be compared to $\varGamma_\rho \sim 150$ MeV. Old analyses of the nucleon FF had already found a similar discrepancy [2].

The anomalous width, mainly related to the real part, turns out to be independent of the choice of the τ parameter within an order of magnitude. It cannot be due to the bin width, whose contribution is added quadratically and is relatively small in the ρ case. On the other hand, as was mentioned previously, the ρ width was recovered in the case of the pion FF.

Concerning the strange, polarized content of the nucleon, there is no evidence of a bump at the $\varPhi$ mass, even if integrated on the bin width. If indeed the strange content of the nucleon is $\int \mathrm{d}Q^2(|G_M^{\rm s\bar{s}}|/|G_M|)^2 \sim 0.15 \div 0.2$, it should be quite visible, concentrated mainly in the $\varPhi$ mass bin. However, for a more quantitative statement to be made, the anomalous ρ width should be understood.

In Fig. 3, the phase of the proton magnetic FF is shown, the spectral function and other plots are reported elsewhere [31]. Above ~ 2 GeV, the phase is ~ 390 degrees, to be compared to the expected asymptotic value of 360 degrees [27].

In Fig. 1b the proton space-like magnetic FF data are compared with the expectation from the solution of the DR on $\log G(Q^2)$. The hypothesis there are no zeros on

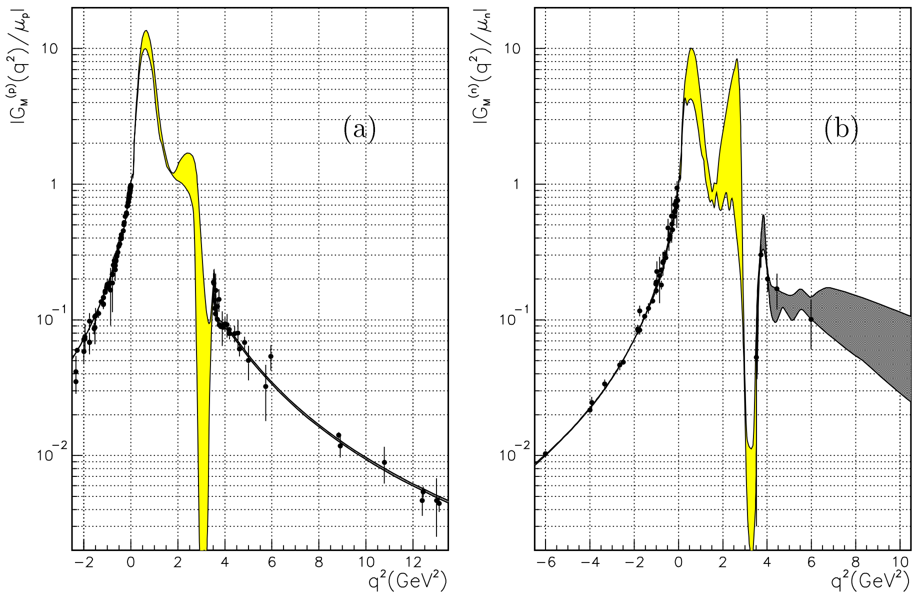

Fig. 4a,b. Proton **a** and neutron **b** magnetic form factor according to (6)

the physical Q^2 sheet may be questioned. Yet, once the imaginary part was achieved, a remarkable, nontrivial test was performed [31]: Space-like FF data and the calculation by means of DR involving this imaginary part are in good agreement, at least at low Q^2 (as is expected if there is no zero). Imposing full agreement does not produce significant changes. Of course, a conspiracy by a suitable set of zeros, restoring the ρ width, cannot be excluded.

4 The nucleon isovector time-like magnetic FF

To obtain $G_M^{\rm V}$, the nucleon isovector FF, and $G_M^{\rm S}$, the isoscalar one, the neutron FF has to be considered as well. As was mentioned above, the neutron time-like FF have been measured through only one experiment. The neutron magnetic FF has been derived [16] under the hypothesis that the neutron electric FF in the time-like region is much smaller than the magnetic one, just as it is for space-like region. In fact, data are consistent with an anisotropic angular distribution. The DM2 measurement [28] of the Λ FF leads to results in very good agreement with FENICE, assuming U-spin invariance [29] and a Λ electric FF that is also negligible. The relationship $G_M(4M_n^2) = G_{\rm E}(4M_{\rm n}^2)$ should imply that, just at threshold, also the neutron magnetic FF vanishes. This assumption, relevant very near threshold only, has been considered in the following. In Fig. 1c, the neutron space-like magnetic FF data are compared with the expectation from the solution of the DR on $\log G(Q^2)$. The neutron magnetic FF in the unphysical region, as obtained by our procedure, is reported in Fig. 4b.

The hypothesis that the FENICE data are wrong by a factor of ~ 2 has been simulated, and the results are that the height of the ρ' resonance for the neutron is higher than the height of the ρ' resonance for the proton [31]. Therefore, the apparent anomaly in the FENICE data (the neutron FF are not smaller than the proton FF) would still be there, but shifted to another energy range.

$G_M^{\rm V}$ and $G_M^{\rm S}$ are derived from the aforementioned proton and neutron FF, and the imaginary part of $G_M^{\rm V}$ is shown in Fig. 5a. $|G_M^{\rm V}|$ at its peak and its imaginary part have been derived from the extended unitarity relation, using pion FF data and analytic continuation of the πN scattering amplitude, up to $Q^2 \sim 0.8\,{\rm GeV}^2$ [8,9] (solid line in Fig. 5a). Our result is in good agreement with this expectation.

With a view toward exposing possible common patterns in the near vicinity of the threshold, we have satisfactorily compared a suitable linear combination of $(G_M^{\rm V})^2$ and $(G_M^{\rm S})^2$ [31] to the various measurements of the total σ ($e^+e^- \to$ hadrons) cross section [24], taking into account the Q^2 bin width.

In Fig. 5b, the imaginary part of $G_M^{\rm S}$ is shown. There is a peak at the ω mass, whose half width is compatible with the bin width, and remarkably, the imaginary part of $G_M^{\rm S}$ becomes different from zero at higher Q^2 than $G_M^{\rm V}$, as expected.

There are predictions also for $G_M^{\rm S}$. For instance, chiral perturbation theory suggests that the imaginary part of $G_M^{\rm S}$ is small up to $Q^2 \sim 0.5\ GeV^2$ [30]. However, given that $G_M^{\rm S}$ comes from a difference and given also its sensitivity to the bin width, the isoscalar sector is more affected by the regularization procedure and thus demands further work [31].

The fact that the total areas of the imaginary parts are equal to zero is in agreement with the superconvergence expectation.

Conclusions

The nucleon time-like magnetic FF in the unphysical region has been obtained in an almost model-independent

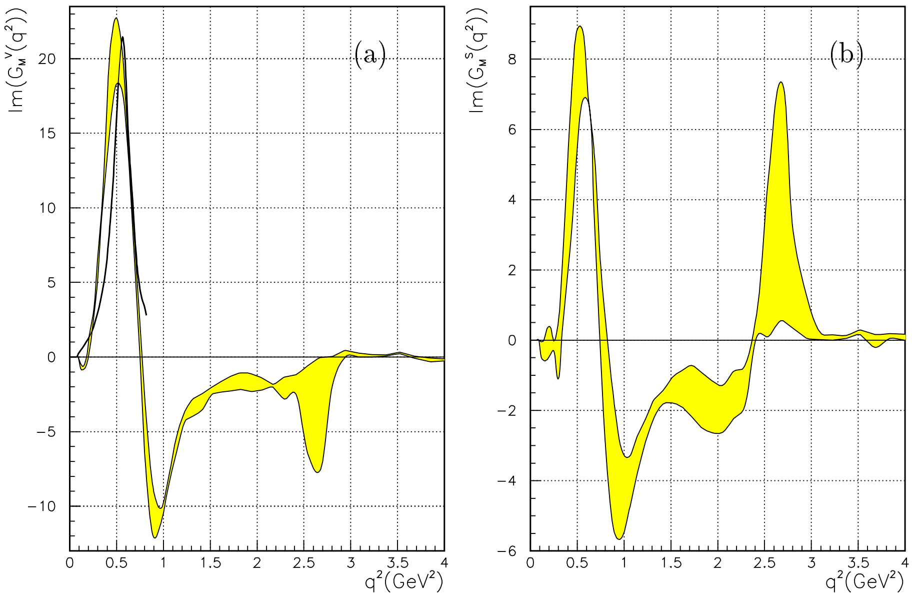

Fig. 5a,b. Imaginary part of the nucleon magnetic isovector **a** and isoscalar **b** form factor. Expectation from unitarity relation is also shown in **a**

way by means of a DR for $\log|G(Q^2)|$, using space-like and time-like data together with a regularization method.

Resonances have been found to be consistent with the $\rho(770)$ and $\rho'(1600)$ masses. However, a very large ρ width is obtained. This result is reminiscent models in which mesons are different from baryons. No evidence has been found for a sizeable Φ contribution; this is contrary to what is expected if there is indeed a large polarized strange content in the nucleon. This work, which aims toward the understanding of the sources of the discrepancies between our conclusions and other dispersion analyses, as well as evaluations by means of the unitarized VDM, is in progress.

Acknowledgements. We warmly acknowledge the FENICE Collaboration and D. Drechsel, U. Meißner, and M. Karliner for their important remarks.

References

1. M.Gourdin, Phys. Rep. 11, No. 2 (1974) 29.
2. J.S.Ball, D.Y.Wong Phys. Rev. 130 (1963) 2112; M.W.Kirson Phys. Rev. 132 (1963) 1249; J.S.Levinger, C.P.Wang, Phys. Rev. 136 (1964) B733; J.S.Levinger, C.P.Wang, Phys. Rev. 138 (1965) B1207; B.Orman, Phys. Rev. 138 (1965) B1308; B.Orman, Phys. Rev. 145 (1966) 1140.
3. G.F.Chew et al., Phys. Rev. 110 (1958) 265; P.Federbush, M.L.Goldberger, S.B.Treiman, Phys. Rev. 112 (1958) 642; S.D.Drell, F.Zachariasen, E.m. Structure of Nucleons (Oxford Univ.Press, Oxford, 1960); J.S.Levinger, R.F.Peierls, Phys. Rev. 134 (1964) B1314; G.L.Kane, R.A.Zdanis, Phys. Rev. 151 (1966) 1239; F.Chilton, F.J.Uhrhane, Bull. Am. Soc. 11 (1966) 396;
4. R.Gatto, N.Cabibbo, Phys. Rev. 124 (1961) 1577; V.Wataghin, Nucl. Phys. B10 (1969) 107; J.C.Korner, M.Kuroda, Phys. Rev. D16 (1977) 2165; P.Cesselli, M. Nigro, C. Voci, Proc. of Workshop on Lear Physics Erice (1982); M.Van Der Velde, M.I.Polikarpov, Jour. Nucl. Phys. 35 (1982) 180; E.Etim, A.Malecki, LNF-89-023 (1989); M.M.Giannini, E.Santopinto, M.I.Krivoruchenko, Proceed. Int. Conf. on Meson and Nuclei at Interm. Energies, Dubna, 1994.
5. S.Dubnička, Nuovo Cimento A104 (1991) 1075; S.Dubnička, A.Z.Dubničkova, P.Strizener Nuovo Cimento A106 (1993) 1253.
6. J.Ellis, M.Karliner, H.Kowalski, Phys. Lett. B235 (1990) 341; G.Holzwarth, Z. Phys. A356 (1996) 339.
7. T.H.R.Skyrme, Nucl. Phys. 31 (1962) 556.
8. G.Höhler et al., Nucl. Phys. B114 (1976) 505.
9. H.W.Hammer, U.G.Meißner, D.Drechsel, Phys. Lett. B385 (1996) 343.
10. A.Z.Dubničkova, presented at the LNF Spring School 1998.
11. H.Forkel, Prog. Part. Nucl. Phys. 36 (1996) 229. P.Mergell, U.-G. Meißner, D. Drechsel, Nucl. Phys. A596 (1996) 367.
12. J.E.Bowcock, W.N.Cottingham, J.G.Williams, Nucl. Phys. B3 (1967) 95.
13. V.Blobel, Lectures given at the 1984 CERN School of Computing; A.Höcker, V.Kartvelishvili, MC-TH-95/15, LAL-95/55; E.T.Janes, Proc. IEEE 70 (1982) 939; S.F.Gull, J.Skilling, Proc. IEEE 131 (1984) 1; J.Antolin, A.Cruz, Journ. Math. Phys. 27 (1986) 104.
14. G.Bassompierre et al., Phys. Lett. B68 (1977) 477; B.Delcour et al., Phys. Lett. B86 (1979) 395; D.Bisello et al., Z. Phys. C48 (1990) 23; T.A.Armstrong et al., Phys. Rev. Lett. 70 (1992) 1212; A.Antonelli et al, Phys. Lett. B334 (1994) 431; E835 coll., presented at Hadron97 (August 1997).
15. G.Bardin et al., Nucl. Phys. B411 (1994) 3.
16. A.Antonelli et al, Phys. Lett. B313 (1993) 283; A.Antonelli et al., Nucl. Phys. B517 (1998) 3.
17. V.L.Chernyak, A.R.Zhitnitsky, Nucl. Phys. B246 (1984) 52.
18. S.J.Brodsky, Nucleon Structure Workshop (Frascati, October 1988); T.Hyer, Phys. Rev. D47 (1993) 3875.

19. FENICE Coll. and P.Patteri, πN newsletters 12 (1997) 73; R.Baldini Ferroli, E.Pasqualucci, C.Bini, P.Patteri, Nucl. Phys. 56A (1997) 275.
20. H.Genz, G.Höhler, Phys. Lett. B61 (1976) 389; R.L.Jaffe, Phys. Lett. B229 (1989) 275; J.Ellis, M.Karliner, Phys. Lett. B341 (1995) 397.
21. T.P.Cheng, R.Dashen, Phys. Rev. Lett. 26 (1971) 594; T.P.Cheng, Phys. Rev D13 (1976) 2161; J.F.Donoghue, C.R.Nappi, Phys. Lett. B168 (1986) 105; J.Gasser, H.Leutwyler, M.E.Sainio, Phys Lett B253 (1991) 252; W.Kluge, Prog. Part. Nucl. Phys. 36 (1996) 239. M.J.Alguard et al, Phys. Rev. Lett. 66 (1991) 70.
22. V.A.Matveev, R.M.Muradyan, A.N. Tavkhelidze, Lett. Nuovo Cim. 7,15 (1973) 719; S.J.Brodsky, G.R.Farrar, Phys. Rev. Lett. 31 (1973) 1153; S.J.Brodsky, G.R.Farrar, Phys. Rev. D11 (1975) 1309; S.J.Brodsky, P.G.Lapage, Phys. Rev. D22 (1980) 2157.
23. E.C.Titchmarsch, The theory of functions. London, Oxford University Press 1939; A.A.Logunov, N. van Hieu, I.T. Todorov, Ann. Phys. (NY) 31 (1965) 203.
24. A.Antonelli et al, Phys. Let. B365 (1996) 427.
25. D.Bridges et al., Phys. Lett. B180 (1986) 315; P.Kroll, W.Schweiger, Nucl. Phys. A503 (1989) 865; O.D.Dalkarov et al., Phys. Lett. B392 (1997) 229.
26. A.Z.Dubničkova, S.Dubnička, M.P.Rekalo, Z. Phys. C70 (1996) 473.
27. R.Baldini, C.Bini, E.Luppi, Phys. Lett. B404 (1997) 362.
28. D.Bisello et al., Nuc. Phys. B224 (1983) 379, LAL 88-58 (1988).
29. M.E.Biagini, L.Cugusi, E.Pasqualucci, Z. Phys. C52 (1991) 631 .
30. U.-G.Meißner, Nucl. Phys. A623 (1997) 340.
31. R. Baldini, S. Dubnička, P. Gauzzi, S. Pacetti, E. Pasqualucci, Y. Srivastava, LNF98/024(P).